View metadata, citation and similar papers at core.ac.uk
brought to you by CORE
provided by RERO DOC Digital Library

Appl. Phys. B 81, 1049–1052 (2005)
DOI: 10.1007/s00340-005-1964-5
Applied Physics B
Lasers and Optics
Rapid communication

S.V. MARCHESE[1,✉]
E. INNERHOFER[1]
R. PASCHOTTA[1]
S. KURIMURA[2]
K. KITAMURA[2]
G. ARISHOLM[3]
U. KELLER[1]

Room temperature femtosecond optical parametric generation in MgO-doped stoichiometric $LiTaO_3$

[1] ETH Zurich, Physics Department/Institute of Quantum Electronics, Wolfgang-Pauli-Strasse 16, 8093 Zurich, Switzerland
[2] National Institute for Material Science, Namiki 1-1, Tsukuba 305-0044, Japan
[3] FFI (Norwegian Defence Research Establishment), Postboks 25, NO-2027 Kjeller, Norway

Received: 19 July 2005
Published online: 3 November 2005 • **© Springer-Verlag 2005**

ABSTRACT We demonstrate room temperature femtosecond optical parametric generation with high average output power in periodically poled MgO-doped stoichiometric $LiTaO_3$. Direct pumping with 725-fs pulses from a passively mode-locked thin disk laser at 1030 nm resulted in stable 1.5 W average signal power at 1484 nm at the full laser repetition rate of 59 MHz. With this demonstration we achieved a significant simplification of our recently presented red-green-blue laser source because no temperature stabilization of any nonlinear crystal is required.

PACS 42.65.Yj; 42.70.Mp; 42.79.Nv

1 Introduction

Optical parametric generators (OPG) based on periodically poled ferroelectric crystals have been shown to be attractive sources of wavelength-tunable ultrashort pulses. Compared to synchronously pumped parametric oscillators, they are simpler and more robust, since synchronized cavities are not required. They do, however, require high pump pulse energies to exceed the threshold for parametric generation and must be operated with high parametric gain (order of 100 dB) for efficient conversion. Recent development of high average power passively mode-locked thin disk lasers [1, 2] allowed to reach this level of parametric gain without amplification of the laser pulses, so that a parametric generator can be driven at the full laser repetition rate of several tens of megahertz.

Single-pass femtosecond OPG at 35 MHz has previously been demonstrated in periodically poled lithium niobate (PPLN), where tunability of the signal output has been obtained in the broad range of 1.38–1.56 μm using different poling periods and crystal temperatures [3]. Pumped with 0.6-ps pulses from a passively mode-locked Yb:YAG thin disk laser at 1030 nm, the PPLN generated pulses with a duration of 307 fs. The average signal power was limited to 0.5 W by the damage in the congruent material. Better performance was later achieved using periodically poled stoichiometric lithium tantalate (PPSLT), which has a higher damage threshold [4]. In that experiment, 300-fs pulses at 1030 nm from a passively mode-locked Yb:KYW thin disk laser were used at a repetition rate of 24 MHz, yielding stable 1 W average signal power in 320-fs pulses. Compared to stoichiometric $LiNbO_3$ (SLN), the lower coercive field of stoichiometric $LiTaO_3$ (SLT) allows high quality domain switching even in thicker crystals [5]. This makes it a favorable material for high power applications, where large mode areas are required to avoid crystal damage. In another approach, 7-ps pulses from an 82-MHz oscillator-amplifier system were used to generate 6.3 W of average signal power in a PPLN crystal [6]. Here, the use of longer pulses allowed efficient conversion and higher average pump power at moderate peak intensities inside the crystal. To avoid photorefractive damage, the crystals in all the mentioned experiments were operated at an elevated temperature in temperature-stabilized ovens. This temperature elevation has long been a requirement for periodically poled crystals, adding complexity to the otherwise simple setup of an OPG. Higher resistance to photorefractive damage and green-induced infrared absorption has been observed and investigated in MgO-doped SLN (Mg:SLN) [7, 8] and more recently, efficient optical parametric oscillation could be demonstrated at room temperature in MgO-doped SLT (Mg:SLT) [9]. Another advantage of Mg:SLT is the expected higher thermal conductivity due to a reduced defect density and lower operation temperature, which reduces the thermal disturbance of phase matching caused by absorption.

Here we present the optical parametric generation in a periodically poled Mg:SLT (PPMgSLT) crystal, operated at room temperature without temperature stabilization. Pumped with 6.4 W from a passively mode-locked Yb:YAG thin disk laser at 1030 nm, the OPG delivers stable 1.5 W average signal power at 1484 nm using the full laser repetition rate of 59 MHz. The idler wavelength (not measured) is 3.37 μm, and some green light at 515 nm arises from second-harmonic generation (SHG) because the poling period is close to the one for fourth-order quasi-phase-matched SHG. With higher pump power

✉ Fax: +41-44-633-10-59, E-mail: marchese@phys.ethz.ch

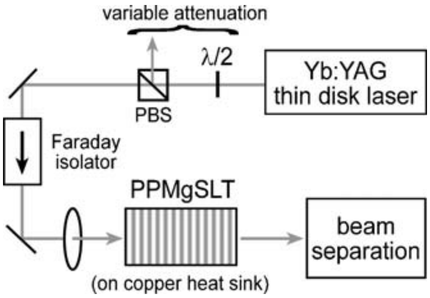

FIGURE 1 Schematic representation of the experimental setup. $\lambda/2$: half-wave plate; PBS: polarizing beam splitter; PPMgSLT: periodically poled MgO-doped SLT crystal mounted on a copper heat sink

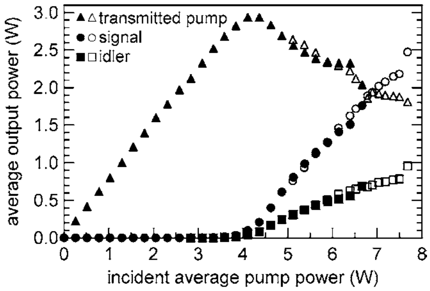

FIGURE 2 Average output powers of signal, idler and transmitted pump versus average pump power incident on the crystal. Filled and open symbols correspond to two measurements at different crystal positions

(7.7 W), we achieved even 2.4 W of signal power for a few minutes, before damage occurred.

2 Experimental setup

We used a laser setup similar to the one described in [10]. The laser generated up to 50 W in 725-fs pulses. After passing a variable attenuator and a Faraday isolator, the pump beam was focused to a 34-μm radius inside the 30-mm long PPMgSLT crystal (Fig. 1). The size of the focus was chosen such that we operated near the optimum focusing condition derived in [11]. The referenced model neglects depletion of the pump and only treats a time-independent situation. However, numerical simulations have shown that the optimum focusing condition is similar for our case with strong pump depletion and pulsed operation.

The uncoated crystal has a thickness of 1 mm and an MgO doping concentration of 1 mol %. The periodically poled region is 2 mm wide and consists of a single 30-μm poling period. The crystal is mounted on a copper heat sink for passive cooling.

3 Experimental results

Pumped with 6.4 W incident on the entrance face, we obtained 1.5 W average signal power and 0.6 W idler power. At this power level, the OPG operated stably with a calculated pump peak intensity of 6.3 GW/cm^2 inside the crystal, assuming no significant conversion at the position of the focus. The parasitic green light had an average power of 0.18 W. The total conversion efficiency from pump to signal and idler is 33%. Taking into account the losses due to Fresnel reflections at the crystal's uncoated surfaces, the total internal conversion efficiency is $\approx$ 43%. Here we used a reported Sellmeier equation for undoped SLT [12] to calculate the reflection losses for the various wavelengths.

Figure 2 shows the measured output powers of signal and idler and the transmitted pump power as functions of the incident pump power. Filled and open symbols correspond to measurements with the beam at two different transverse positions in the crystal, because damage occurred within a few minutes at the first position at an average signal power of 1.75 W, where the corresponding peak pump intensity inside the crystal was 6.6 GW/cm^2. We believe that the pump (and not the signal or idler) intensity is relevant for damage, since damage was observed near the beam focus, where signal and idler powers are small. In the second measurement, 2.4 W signal and 1 W idler power were reached with an incident pump power of 7.7 W. This translates into a total conversion efficiency of 43%, and an internal conversion efficiency of $\approx$ 58%.

At 1.5 W average signal power, the triangular shape of the measured intensity autocorrelation indicates a distortion of the temporal pulse shape (Fig. 3). This distortion is due to the combined action of pump depletion and temporal

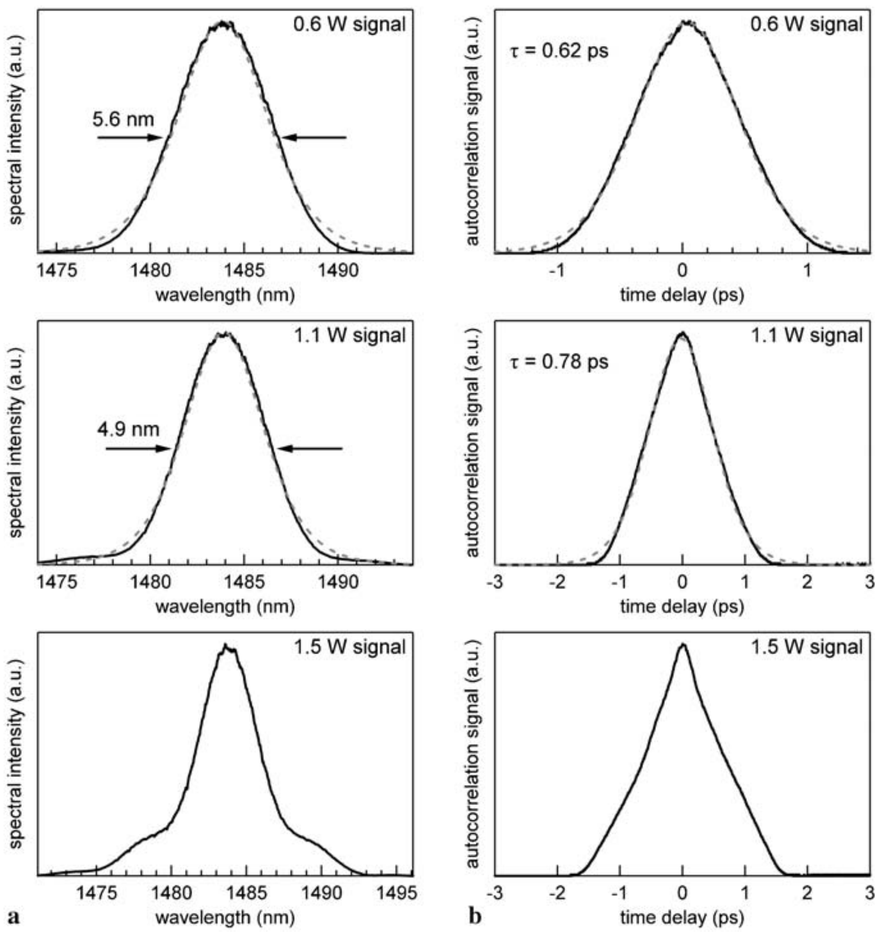

FIGURE 3 Optical spectrum (**a**) and intensity autocorrelation (**b**) of the measured signal pulses for 0.6 W, 1.1 W and 1.5 W of average signal output power

walk-off between the pump and signal pulse resulting from the group velocity mismatch (GVM) inside the PP-MgSLT crystal (see below). At 0.6 W signal power the distortions are not yet observed, and we obtained a FWHM pulse duration of 0.62 ps using a $sech^2$ fit. With a FWHM spectral bandwidth of 5.6 nm, the time-bandwidth product is 0.47. At 1.1 W average signal power, the influence of GVM on the temporal pulse shape starts to become visible in the autocorrelation. Here we estimated a pulse duration of 0.78 ps. The spectral bandwidth was 4.9 nm, leading to a time-bandwidth product of 0.52.

Using a knife-edge method, we measured the beam quality at average signal powers of 0.6 W, 1.1 W, and 1.5 W with resulting M^2 values of 1.25, 1.4, and 1.6, respectively. This reduction in beam quality with increasing conversion efficiency is typical for high gain optical parametric systems [13].

4 Numerical simulations

We further investigated the influence of the GVM using an advanced numerical simulation model, which takes into account the full spatial and temporal nature of the nonlinear interaction and exact dispersion [14]. To simulate the quantum noise, from which the OPG starts, the model uses signal and idler inputs with numerically generated fluctuations. The GVM enters the model by using the Sellmeier equations from [12] to calculate the wavelength dependencies of the refractive indices. The best agreement with the experiment was achieved using an effective nonlinearity of $d_{eff} \approx 10\,pm/V$. The influence of the GVM on the amplification process depends on the relative walk-off of the signal and idler with respect to the pump. Neglecting conversion, a pump and signal pulse simultaneously entering the crystal would exit the crystal with a time separation of ≈ 2.5 ps due to the GVM of ≈ 83 fs/mm. Signal and idler walk off in opposite directions relative to the pump. This is a favorable condition that allows high gain even if the walk-off time for linear pulse propagation is longer than the pulse length [15]. In the regime with low conversion, the strong temporal gain guiding by the pump pulse can produce high-quality signal and idler pulses, which overlap well with the pump pulse. When the pump pulse becomes depleted, its peak will shift in time, and the resulting change of the temporal gain guiding can distort the generated pulses. In Fig. 4, this is demonstrated using the signal pulses retrieved from the simulation at signal output powers of 0.6 W, 1.1 W and 1.5 W. The intensity autocorrelations calculated from these pulses show good qualitative agreement with the measured intensity autocorrelations in Fig. 3b. As can be seen the generated signal pulses have durations similar to the pump pulse, despite the temporal walk-off between signal and pump which is much larger than the pulse durations. For even higher pump power, backconversion can cause further distortion and finally, these effects lead to two distinct peaks in the temporal pulse profile when simulating the highest experimentally achieved average signal power of 2.4 W (Fig. 5).

Using a shorter crystal would reduce the influence of the GVM and allow for better temporal pulse shape. However, reducing the crystal length also reduces the gain of the OPG. Because the pump beam in the 30-mm long crystal is already focused to near optimum radius for efficient conversion, the reduced gain due to the smaller crystal length could not be compensated for by tighter focusing. This was confirmed in simulations with a 25-mm long crystal, where similar conversion with equal pump power could not be achieved even with optimized tighter focusing. Furthermore, a smaller focus would lead to higher intensities increasing the risk of crystal damage. Hence the use of relatively long crystals with optimum focusing appears to be the only feasible solution to achieve sufficient gain for high conversion in a femtosecond OPG, despite the significant temporal walk-off.

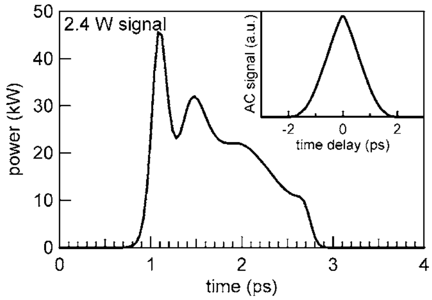

FIGURE 5 The temporal pulse shape of the simulated signal pulse at 2.4 W average signal power shows two distinct peaks. The shape of the intensity autocorrelation (*inset*) characteristic to such a pulse was also observed in the experiment

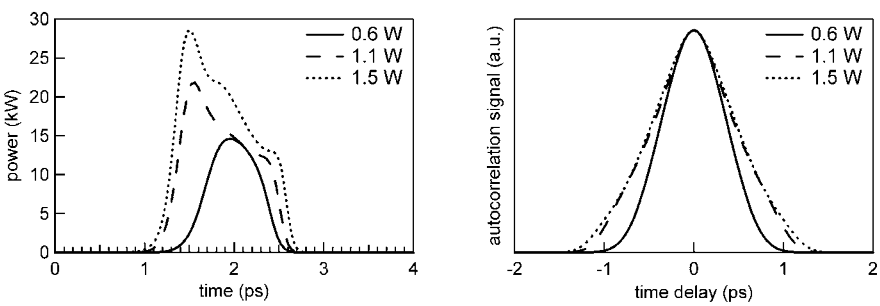

FIGURE 4 Time-dependent power (*left*) of the pulses retrieved from simulations with average signal output powers of 0.6 W (*solid*), 1.1 W (*dashed*) and 1.5 W (*dotted*). The temporal distortion leads to a triangularly shaped intensity autocorrelation (*right*)

5 Conclusions

In conclusion, we have demonstrated stable and efficient room temperature femtosecond optical parametric generation with a high average signal output power of 1.5 W at the full laser repetition rate of 59 MHz. Measurement and simulations show that the generated pulses have durations similar to those of the pump pulses despite the influence of the large GVM. Operation without the temperature-stabilized oven is a significant step towards simpler OPG devices for real world applications. Furthermore, it will simplify our recently presented red-green-blue (RGB) system [10], because all nonlinear crystals can now be operated at room temperature. The system will then no longer require any temperature-stabilized oven, which is an additional advantage for a commercial high power RGB source.

REFERENCES

1 F. Brunner, T. Südmeyer, E. Innerhofer, R. Paschotta, F. Morier-Genoud, J. Gao, K. Contag, A. Giesen, V.E. Kisel, V.G. Shcherbitsky, N.V. Kuleshov, U. Keller: Opt. Lett. **27**, 1162 (2002)

2 E. Innerhofer, T. Südmeyer, F. Brunner, R. Häring, A. Aschwanden, R. Paschotta, U. Keller, C. Hönninger, M. Kumkar: Opt. Lett. **28**, 367 (2003)

3 T. Südmeyer, J. Aus der Au, R. Paschotta, U. Keller, P.G.R. Smith, G.W. Ross, D.C. Hanna: J. Phys. D: Appl. Phys. **34**, 2433 (2001)

4 T. Südmeyer, F. Brunner, R. Paschotta, U. Keller, T. Usami, H. Ito, M. Nakamura, K. Kitamura: Conference on Laser and Electro-Optics CLEO 2002, Talk CTuO4 (2002)

5 K. Kitamura, Y. Furukawa, K. Niwa, V. Gopalan, T.E. Mitchell: Appl. Phys. Lett. **73**, 3073 (1998)

6 B. Köhler, U. Bäder, A. Nebel, J.-P. Meyn, R. Wallenstein: Appl. Phys. B **75**, 31 (2002)

7 Y. Furukawa, K. Kitamura, S. Takekawa, K. Niwa, H. Hatano: Opt. Lett. **23**, 1892 (1998)

8 Y. Furukawa, K. Kitamura, A. Alexandrovski, R.K. Route, M.M. Fejer, G. Foulon: Appl. Phys. Lett. **78**, 1970 (2001)

9 N.E. Yu, S. Kurimura, Y. Nomura, M. Nakamura, K. Kitamura: Appl. Phys. Lett. **85**, 5134 (2004)

10 F. Brunner, E. Innerhofer, S.V. Marchese, T. Südmeyer, R. Paschotta, T. Usami, H. Ito, S. Kurimura, K. Kitamura, G. Arisholm, U. Keller: Opt. Lett. **29**, 1921 (2004)

11 G.D. Boyd, D.A. Kleinmann: J. Appl. Phys. **39**, 3597 (1968)

12 A. Bruner, D. Eger, M.B. Oron, P. Blau, M. Katz, S. Ruschin: Opt. Lett. **28**, 194 (2003)

13 G. Arisholm, R. Paschotta, T. Südmeyer: J. Opt. Soc. Am. B **21**, 578 (2004)

14 G. Arisholm: J. Opt. Soc. Am. B **16**, 117 (1999)

15 R. Danielius, A. Piskarskas, A. Stabinis, G.P. Banfi, P. Di Trapani, R. Righini: J. Opt. Soc. Am. B **10**, 2222 (1993)